J|A|C|S COMMUNICATIONS

Published on Web 11/02/2009

Low Temperature CO Oxidation over Supported Ultrathin MgO Films

Anders Hellman, Simon Klacar, and Henrik Grönbeck*

Competence Center for Catalysis and Department of Applied Physics, Chalmers University of Technology, SE-412 96 Göteborg, Sweden

Received August 13, 2009; E-mail: ghj@chalmers.se

Carbon monoxide oxidation over noble metal surfaces is a prototypical reaction within heterogeneous catalysis. Based on experiments at ultrahigh vacuum,[1] the reaction is generally assumed to proceed via a Langmuir−Hinshelwood mechanism where adsorbed CO reacts with dissociated O_2 to form CO_2. At higher partial pressures of O_2, it has been suggested that the formation of surface oxides may be of importance at certain reaction conditions.[2,3] The scientific interest in CO oxidation is motivated by its immense technological importance. One example is the three-way catalyst (TWC) used for emission control of gasoline fueled vehicles. In this catalyst, the active material is nm-sized noble metal (Rh, Pd, Pt) particles dispersed on an oxide. Platinum is, in this application, often used for oxidation of carbon monoxide and hydrocarbons. One severe limitation of the TWC, however, is the reduced activity at low temperatures, generally referred to as the cold-start problem.[4] The issue arises as CO has a higher sticking probability than O_2 on Pt and, moreover, the desorption rate of CO is moderate at low temperatures (the CO−metal adsorption energy is too high). At low temperatures, CO blocks all metal sites and poisons the catalyst. Catalyst ignition does not occur until the metal particles have been heated to sufficiently high temperatures by the exhaust gas. Over the years, the cold-start problem has been addressed by suggestions of catalyst formulations that resist CO poisoning. Recent examples are Au nanoparticles supported on base transition metaloxides,[5] nanosized Co_3O_4,[6] and monolayer FeO films grown on Pt(111).[7] In the present Communication we present an inverse catalyst[8] with properties suitable for low temperature CO oxidation. In particular, we show that CO oxidation over ultrathin MgO supported on Ag proceeds with an activation barrier lower than the corresponding barrier on Pt(111). Moreover, the adsorption energy of CO is low enough to prevent CO poisoning.

The density functional theory (DFT) is used in a real space implementation[9] of the projector augmented wave method[10] with the exchange and correlation functional approximated by the Perdew−Burke−Ernzerhof formula.[11] See Supporting Information (SI) for further details.

The calculated enthalpy diagrams for CO oxidation over MgO/Ag(100) (Langmuir−Hinshelwood (HL) or Eley−Rideal (ER) mechanisms) are shown in Figure 1. O_2 adsorbs molecularly in a bridge configuration between two Mg cations with an adsorption energy of 0.82 eV. Adsorption as a dissociated molecule (one O in peroxo configuration and one bridging Mg^{2+}, see SI) is *endothermic* by 1.07 eV with respect to O_2 in the gas phase. CO is bonded by 0.40 eV to the surface with preadsorbed O_2. A slight stabilization of the bond owing to O_2 is predicted; the CO adsorption energy on the bare MgO/Ag surface is calculated to be 0.24 eV. It is mainly the adsorption energy of O_2 that is influenced by the Ag support. The O_2 adsorption energy is only 0.20 eV on unsupported MgO. The corresponding value for CO is 0.12 eV which is in good agreement with previous reports.[12] The activation barrier to form CO_2 from adsorbed CO and O_2 is predicted to be 0.70 eV. The

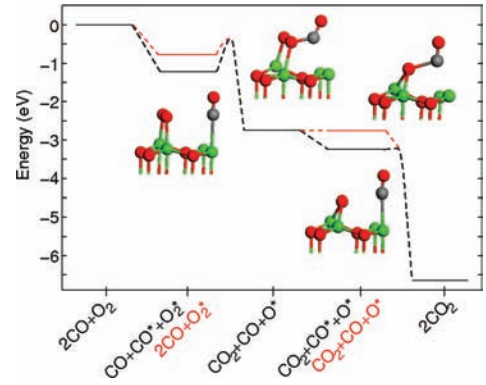

Figure 1. Enthalpy diagram for CO oxidation over MgO/Ag(100). The ER energies are marked by red bars in reaction steps where ER and HL enthalpies differ. Structural models show optimized structures for (O_2 + CO)/MgO/Ag and (O + CO)/MgO/Ag together with transition states. Asterisks denote adsorbed species. Atomic color codes: Green (Mg), red (O), and gray (C).

oxidation reaction is strongly exothermic, and the products (adsorbed O and CO_2 in the gas phase) are 2.75 eV below the reactants. The gas phase reaction ($^1/_2O_2 + CO \rightarrow CO_2$) is calculated to be exothermic by 3.20 eV. The corresponding experimental value is 2.95 eV.[13] CO_2 is bonded to the surface by 0.26 eV, and carbonate formation is not preferred on the terrace (see SI). The second CO molecule is adsorbed by 0.49 eV. The single O atom (that occupy a bridge configuration) on the surface is very reactive, and the barrier to form the subsequent CO_2 molecule is only 0.03 eV. The fact that the CO adsorption energy is lower than the first activation barrier indicates that the reaction proceeds via an ER rather than an LH mechanism. For the ER route, the first barrier is reduced to 0.3 eV and the small barrier to form the second CO_2 vanishes. An ER mechanism has previously been proposed for CO oxidation over anionic gold clusters supported on MgO.[14]

The suggested mechanism for CO oxidation over MgO/Ag(100) is clearly different from the traditional LH view of oxidation over Pt(111); O_2 dissociates readily on Pt, and CO reacts with atomic oxygen. The transition state of this reaction has been investigated by DFT in an implementation with pseudopotentials and plane waves.[15] The barrier was calculated to be 1 eV and analyzed to predominantly originate from the cleavage of the oxygen−metal bond.[15] We have repeated the calculations in ref 15, and the barrier within the present computational approach is 0.90 eV, thus 0.2 eV higher than that on MgO/Ag(100). The barriers on MgO/Ag(100) and Pt(111) are of distinctly different origin. On Pt(111), CO−Pt and O−Pt bonds must be broken for the oxidation to proceed.[15] The adsorption energies of O and CO on Pt(111) are here calculated to be 1.26 and 1.77 eV, respectively. On MgO/Ag(100), the barrier originates mainly from O−O cleavage of an activated O_2 molecule (superoxo species). The low activation barrier in conjugation with

10.1021/ja906865f CCC: $40.75

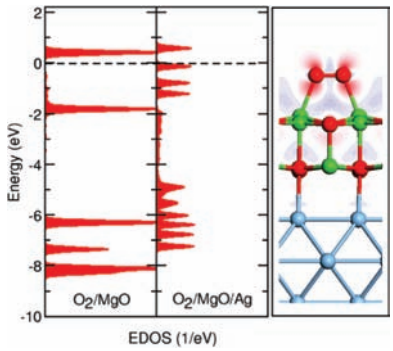

Figure 2. Left: PDOS relative the Fermi energy for O_2 adsorbed onto MgO(100) and MgO/Ag(100) respectively. Right: Charge density difference integrated to a plane perpendicular to the surface for O_2/MgO/Ag shown in the range [−0.9:0.9] e/Å^2. Red (blue) indicates gain (depletion). Atomic color codes same as those in Figure 1 with blue (Ag).

Table 1. Selected Bond Lengths[a]

	d_{O-O}	d_{OO-Mg}	d_{O-O}(TS)	d_{C-O}	d_{CO-Mg}	d_{C-O}(TS)
MgO	1.24	3.50	−	1.14	3.94	−
MgO/Ag	1.32	2.16	1.44	1.14	2.46	1.18

[a] Bond lengths in Å. TS refers to the CO−OO transition state structure.

the weak adsorption energy of CO renders MgO/Ag a promising candidate for low temperature activity.

It has been recognized that thin metaloxide films on metal supports exhibit adsorption properties in variance with the corresponding bulk metaloxides.[16] The modified properties rest in a charge exchange between the adsorbed species and the metal/metal oxide interface. The phenomenon was first predicted for Au atoms adsorbed on MgO/Mo(100)[16a] and later confirmed experimentally via scanning tunneling microscopy measurements on Au atoms supported on MgO/Ag(100).[16b] A similar effect was predicted[16c] and confirmed[16d] for NO_2 adsorption on MgO/Ag(100) and has later been demonstrated to apply for different types of oxides.[16e−g]

The novel catalytic properties of an ultrathin MgO film on Ag(100) originates from the fact that O_2 is activated on the surface. In Figure 2, the electronic density of states projected onto the O_2 states (PDOS) is shown for O_2/MgO and O_2/MgO/Ag. In the case of adsorption on MgO, the $2\pi^*$ state is half-filled and the molecule is a triplet. The situation is different for O_2 adsorption on MgO/Ag(100), where the molecule becomes negatively charged (forming a doublet). This is clearly observed in the PDOS where one initially empty $2\pi^*$ state has moved below the Fermi energy. The charging of the molecule is confirmed by a Bader analysis.[17] For O_2/MgO/Ag(100), O_2 is charged by −0.72 e, MgO by 0.54 e, and Ag by 0.18 e. In Figure 2, we also present the charge density difference map $[\Delta\rho = \rho(O_2/MgO/Ag) - \rho(O_2) - \rho(MgO/Ag)]$. $\Delta\rho$ clearly reveals the charge gain in the $2\pi^*$ state. During the oxidation process of the first CO molecule, the system preserves the doublet spin state; during the transition state, the spin density is transferred to the O atom that remains on the surface. The excess charge on this atom is calculated to be 0.98 electrons.

The activation of O_2 upon adsorption on Ag supported MgO is also observed in structural properties. The O−O bond length (Table 1) is 0.08 Å longer on MgO/Ag as compared to the sole oxide. The C−O bond length is calculated to be similar on MgO and MgO/Ag. This is related to the fact that CO adsorption is only weakly influenced by the support. At the first transition state, the O−O (C−O) bond length is stretched by 0.12 (0.04) Å. The C−O value can be compared to the situation on Pt(111), where it is calculated to be 1.16 Å. The adsorption of O_2 on MgO/Ag(100) induces pronounced structural relaxations in the oxide film. The rumpling is 2% in the MgO/Ag system, whereas it is −17% for O_2/MgO/Ag. The change in rumpling is due to the coordination of Mg cations in the surface layer to the anionic O_2 and a reduced O−Ag distance at the interface. The average O−Ag distance is reduced from 2.65 to 2.46 Å. The large structural relaxations are in agreement with previous results for other adsorbates (see, *e.g.*, 15 g).

In summary, we have demonstrated that a metal supported ultrathin metaloxide is active as a CO oxidation catalyst. In particular, the activation barrier has been predicted to be lower on MgO/Ag(100) than the corresponding barrier on Pt(111). As the adsorption energy of CO is low on MgO/Ag(100), self-poisoning is prevented and the system should be active as a low temperature catalyst. The results may provide a possible interpretation of the recent observation that monolayer FeO(111) films grown on Pt(111) are active for low temperature CO oxidation.[7] The predicted O_2 activation is general in nature, and a high activity can be anticipated for a range of metal−metal oxide combinations. It can, furthermore, be envisioned that inverse catalysts can be tailored for other oxidation reactions.

Acknowledgment. We thank H.-J. Freund, S. Shaikhutdinov, and M. Sterrer for stimulating discussions. Financial support from the Swedish Research Council is acknowledged. The calculations were performed using SNIC resources.

Supporting Information Available: Theoretical procedure, optimized structures, and microkinetic simulations. This material is available free of charge via the Internet at http://pubs.acs.org.

References

(1) Ertl, G.; Engel, T. *Adv. Catal.* **1979**, *28*, 1.
(2) Wang, J. G.; Li, W. X.; Borg, M.; Gustafson, J.; Mikkelsen, A.; Pedersen, T. M.; Lundgren, E.; Weissenrieder, J.; Klikovits, J.; Schmid, M.; Hammer, B.; Andersen, J. N. *Phys. Lev. Lett.* **2005**, *95*, 256102.
(3) Li, W.; Hammer, B. *Chem. Phys. Lett.* **2005**, *409*, 1.
(4) Skoglundh, M.; Fridell, E. *Top. Catal.* **2004**, *28*, 79.
(5) (a) Ishida, T.; Haruta, M. *Angew. Chem., Int. Ed.* **2007**, *46*, 7154. (b) Häkkinen, H.; Landman, U. *J. Am. Chem. Soc.* **2001**, *123*, 9704.
(6) Xie, X. W.; Li, Y.; Liu, Z. Q.; Haruta, M.; Shen, W. J. *Nature* **2009**, *458*, 746.
(7) Sun, Y.-N.; Qin, Z.-H.; Lewandowski, M.; Carraso, E.; Sterrer, M.; Shaikhutdinov, S.; Freund, H.-J. *J. Catal.* **2009**, *359*, 266.
(8) Schoiswohl, J.; Surnev, S.; Netzer, F. P. *Top. Catal.* **2005**, *91*, 36.
(9) (a) Mortensen, J. J.; Hansen, L. B.; Jacobsen, K. W. *Phys. Rev. B* **2005**, *71*, 035109. (b) https://wiki.fysik.dtu.dk/gpaw.
(10) Blöchl, P. E. *Phys. Rev. B* **1994**, *50*, 17953.
(11) Perdew, J. P.; Burke, K.; Ernzerhof, M. *Phys. Rev. Lett.* **1996**, *77*, 3865.
(12) (a) Pacchioni, G. *Surf. Rev. Lett.* **2000**, *7*, 277. (b) Qui, C. *Chem. Phys. Lett.* **2008**, *460*, 457.
(13) *CRC Handbook of Chemistry and Physics*, 89st ed.; Lide, D. R., Ed.; CRC Press, Inc.: Boca Raton, FL, 2008−2009.
(14) Pacchioni, G.; Sicolo, S.; Di Valentin, C.; Chiesa, M.; Giamello, E. *J. Am. Chem. Soc.* **2008**, *130*, 8690.
(15) Alavi, A.; Hu, P.; Deutsch, T.; Silvestrelli, P. L.; Hutter, J. *Phys. Rev. Lett.* **1998**, *80*, 3650.
(16) (a) Pacchioni, G.; Giordano, L.; Baistrocchi, M. *Phys. Rev. Lett.* **2005**, *94*, 226104. (b) Sterrer, M.; Risse, T.; Pozzoni, U. M.; Giordano, L.; Heyde, M.; Rust, H.-P.; Pacchioni, G.; Freund, H.-J. *Phys. Rev. Lett.* **2007**, *98*, 096107. (c) Grönbeck, H. *J. Phys. Chem. B* **2006**, *110*, 10268. (d) Starr, D. E.; Weis, C.; Yamamoto, S.; Nilsson, A.; Bluhm, H. *J. Phys. Chem. C* **2009**, *113*, 7355. (e) Broqvist, P.; Grönbeck, H. *Surf. Sci.* **2006**, *600*, L214. (f) Hellman, A.; Grönbeck, H. *Phys. Rev. Lett.* **2008**, *100*, 116801. (g) Frondelius, P.; Hellman, A.; Honkala, K.; Häkkinen, H.; Grönbeck, H. *Phys. Rev. B* **2008**, *78*, 085426.
(17) Henkelman, G.; Arnaldsson, A.; Jónsson, H. *Comput. Mater. Sci.* **2006**, *36*, 354.

JA906865F